Three-Phase Four Wire High-Frequency Link Converter for Residential DC Grids

Pietro Emiliani
Tallinn University of Technology
Dept. of Mechatronics and Electrical Power Engineering
Tallinn, Estonia
piemil@ttu.ee

Andrei Blinov
Tallinn University of Technology
Dept. of Mechatronics and Electrical Power Engineering
Tallinn, Estonia
andrei.blinov@taltech.ee

Giovanni De Carne
Karlsruhe Institute of Technology
Institute for Technical Physics
Karlsruhe, Germany
giovanni.carne@kit.edu

Gabriele Arena
Karlsruhe Institute of Technology
Institute for Technical Physics
Karlsruhe, Germany
gabriele.arena@kit.edu

Dmitri Vinnikov
Tallin University of Technology
Dept. of Mechatronics and Electrical Power Engineering
Tallinn, Estonia
dmitri.vinnikov@taltech.ee

***Abstract*— There is increasing penetration of dc native renewable technologies, such as batteries and photovoltaics in the distribution grid. These renewable technologies can be interconnected with dc microgrids, which in turn often have a bidirectional connection with the ac distribution grid to enable energy exchange. For safety reasons, this connection is often galvanically isolated with a transformer. This paper presents a single stage high frequency link converter, based on an indirect matrix converter. A three leg four wire configuration is proposed to be able to operate in unbalanced conditions and provide various ancillary grid services. A digital controller is developed to control the grid currents and eliminate distortion at the zero crossing of the matrix converter. The results are verified with a PSIM model.**

Keywords—dc/ac, galvanic isolation, inverters, high frequency link conversion, power factor correction, ancillary grid services

I. INTRODUCTION

Renewable energy sources and technologies for distributed generation, such as photovoltaics and fuel cells, operate natively in dc. Electrical batteries, whether for storage or electric vehicles, are also dc native. Furthermore, most modern loads are supplied in dc, and even inverter-driven motor loads, such as washing machines and electric vacuum cleaners have a dc power stage. The aforementioned devices can be interfaced with a dc microgrid, which is a small, residential scale electric grid that operates in direct current. This eliminates unnecessary power conversion stages and simplifies the control of the microgrid, as there are no problems of synchronization or reactive power [1]-[4]. Both the dc microgrid and ac distribution grid can benefit from a bidirectional ac/dc converter, as shown in Fig. 1.

High-frequency link converters (HFLC) are an emerging alternative solution to two-stage systems [5], that provides bidirectional dc/ac conversion with high frequency isolation. The basic structure is shown in Fig. 2. The dc side is composed of a full bridge that generates a high frequency square wave at the primary of the transformer. The secondary of the transformer is connected to a one by three phase matrix converter, which unfolds and sinusoidally modulates the high frequency voltage,

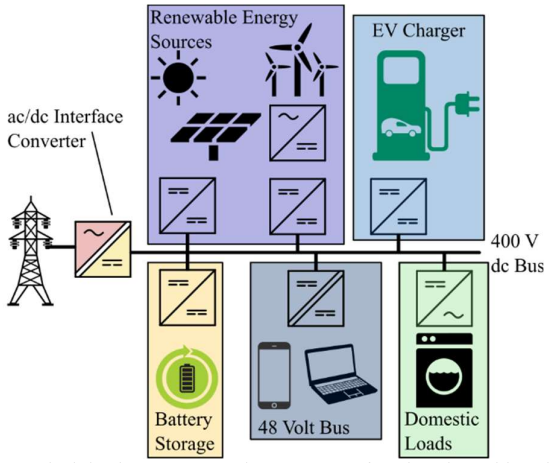

Fig 1. Typical loads, storage, and generators of a dc microgrid and the connection to the ac distribution grid. The ac/dc interface converter must be bidirectional to allow for the microgrid to provide services to the ac grid.

stepping it down to grid frequency. The matrix converter can be seen as two typical inverters, placed 180 degrees out of phase to operate with the opposite input voltages provided by the high frequency link. The bidirectional switches that result from this configuration are four quadrant switches [6]-[9].

Three-phase three-wire inverters feature good semiconductor wafer utilization and high efficiency, as well as high utilization of their dc link. However, the output currents are coupled due to Kirchhoff's current law $i_a + i_b + i_c = 0$ and cannot be independently controlled.

To allow for independent control of the phase currents it is necessary to decouple them by introducing a neutral wire, allowing for unbalanced operation as now $i_a + i_b + i_c = i_n$.

Such operating mode can be desired to provide active phase balancing feature to the ac grid [10], [11]. This paper studies the realization of the neutral wire for use in a high-frequency link converter.

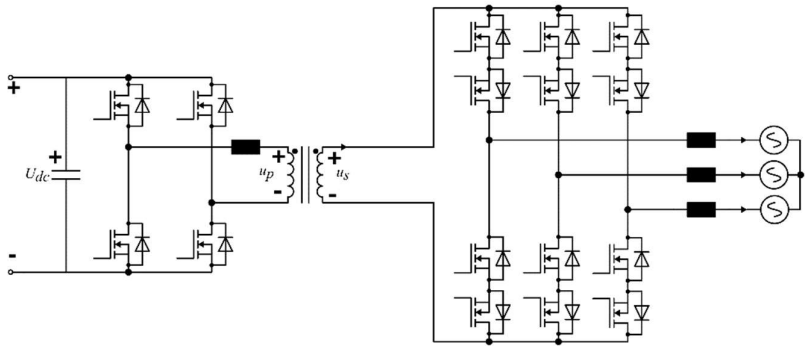

Fig. 2 High frequency link converter. The dc side is a full bridge and the ac side is a 3-1 phase matrix converter that connects to the grid. The dc side switches are denoted with T and the ac side switches are denoted with "S"

II. Converters with a Neutral Wire

With the inclusion of the neutral wire the converter can be seen as three independently controlled half-bridges. However, during unbalanced operation, the power flow will have a 100 Hz ripple dependent on the inverse sequence of the currents, analogous to that found in one phase dc/ac systems.

In the conventional inverter, there are two ways to include the neutral wire. The simpler solution, shown in Fig 3 (a) is to split the dc link and connect the neutral wire to the center of the dc link. This solution comes at the cost of no control over the neutral point, and poor utilization of the dc link. Alternatively, as shown in Fig 3 (b), a fourth active leg can be added to the inverter to control the neutral point, however this requires additional switches, and will introduce additional conduction and switching losses.

Both of these solutions can be extended to the high frequency converter. In the HFLC, the inverters operate with the high frequency link of the transformer, which can be center- tapped to provide a connection to the neutral point. This solution is shown in Fig. 4 (a) and is analogous to the split dc link found in non-isolated converters. The four-leg realization is also possible, shown in Fig 4 (b), however due to the anti-series connection of the switches this would require four additional discrete semiconductors and result in increased conduction losses.

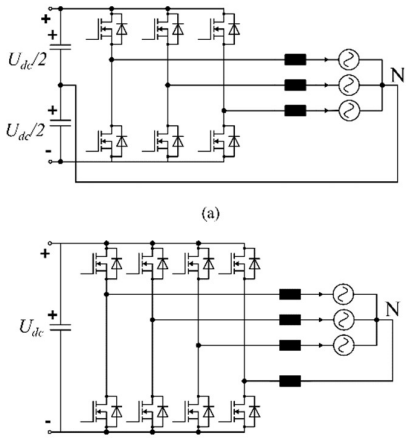

Fig. 3 Two conventional ways to realize three phase four wire converters. In (a) is the split dc link solution and (b) is the four leg solution.

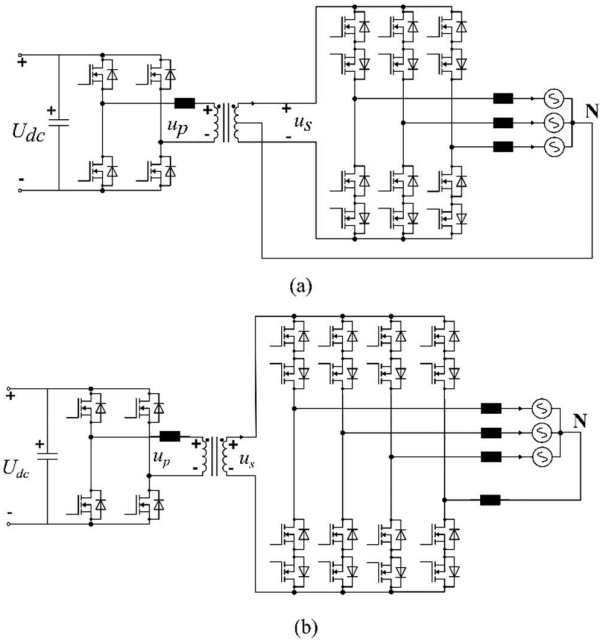

Fig. Fig. 4 The equivalent realizations of four wire converters for the isolated HFLC. In (a) the high frequency link is split by center tapping the transformer, in (b) a fourth controlled leg is introduced to actively control the neutral point.

III. Converter Operation

A. Modulation method

The anti-series connection of the switches introduces some disadvantages to the converter. First is the increased conduction loss, as the current must be conducted by two devices, but also this configuration does not allow for a freewheeling current to pass if the switches are open. If a phase leg of the converter commutates from one high frequency rail to the other under hard switching, the difference between the current of the grid inductor and transformer leakage inductance will provoke massive voltage spikes on the switches. Thus, it is necessary to switch the converter leg with zero current switching to avoid damage to the semiconductor devices [12]. This is possible by introducing a shoot-through state in the converter during which the current is redistributed from top to bottom arm of the converter and vice versa, allowing for safe commutation.

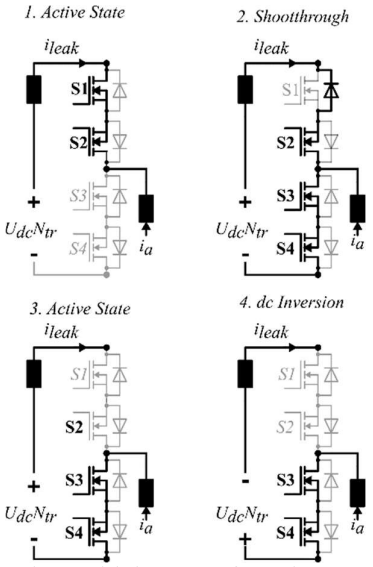

Fig. 5 Converter leg modulation. In a four wire system the legs are independently controlled, so only one leg is shown.

During this shoot-through state, the dc link voltage is imposed on the leakage inductance in such a way that it reverses the phase current through it. The modulation scheme is shown in Fig. 5 and described below in the case of rectifier operation.

1. Switches S_1, S_2 are conducting, connecting the phase leg to the top rail of the HFT. S_1 operates in synchronous rectification and the converter is transferring power from ac to dc side, with negative leakage current.
2. Switches S_3, S_4 turn ON. S_1 is turned OFF but continues to conduct through its body diode. The voltage across the entire leg, i.e., the voltage across the HFT secondary after the leakage inductance, is clamped to zero. The entire secondary voltage falls upon the leakage inductance, and the current through the leakage inductance redistributes from top to bottom arm, limited by the leakage inductance.
3. Once the current has redistributed, and the contribution of the phase current has swapped direction in the leakage inductance, S_1 undergoes reverse recovery and begins blocking the voltage. The secondary of the transformer is no longer clamped and power flows through the converter again. Switch S_2 can now be turned off with zero current switching (ZCS).
4. The dc side polarity is inverted by the commutation of the dc full-bridge; the process can now be repeated for the negative half-wave of the square wave voltage.

One of the consequences of this type of modulation is that the duty cycle of the ac side switches is fixed at 0.5 + overlap time. Therefore, whatever duty cycle is applied to the positive half wave, an equal duty cycle will be applied to the negative half wave. Essentially the two inverters that are 180 degrees out of phase have an interleaved operation, as shown in Fig. 6. This doubles the ripple seen by the filtering components, halving the filtering effort. There is some duty cycle loss during the overlap time, however with low leakage inductance this effect can be neglected.

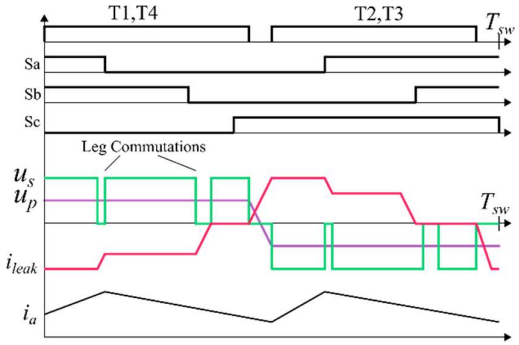

Fig. 6 General representation of converter waveforms. Sa, Sb, and Sc, represent whether the respective phase leg is connected to the top or bottom rail of the high frequency transformer. Because of the dc polarity switch, leg experiences the applied volt-seconds of both the top and bottom high frequency rail twice, doubling the ripple seen by the filter elements.

B. Control method

A predictive digital controller that calculates the required duty cycle for a given change in current is used to control the converter. The system can be seen as the one shown in Fig. 7, assuming turns ratio of 1 n:n. The four quadrant switches select which rail of the HFT connects to the grid. The two voltages represented as dc sources are actually square waves and alternate polarity with a constant duty cycle. The change in phase current during one half-period can be found from the volt-second balance on the grid inductor:

$$\Delta i = \frac{U_{dc} n T_{sw}(2\delta - 1) - U_g T_{sw}}{L}. \tag{1}$$

The duty cycle can then be calculated as

$$\delta = \frac{L\Delta i + U_g T_{sw}}{U_{dc} n T_{sw}} + \frac{1}{2}. \tag{2}$$

C. Ripple on dc Capacitor

The ripple on the dc side capacitors has two contributing factors. The first is the high frequency ripple due to the switching providing discontinuous power to the dc link capacitors, as this occurs at switching frequency, it is easily filtered by relatively small capacitances. This is especially true in the case of the described modulation wherein the switching ripple is actually twice the switching frequency. On the other hand, when operating with unbalanced currents, the negative sequence of the current results in a ripple at twice the fundamental frequency. This requires a significantly greater filtering effort, and the switching ripple is negligible in comparison.

The measure of unbalance in a three phase system can be described with the symmetric components, which are calculated with the Fortescue transform, in the case of three phase currents it is:

$$\bar{I}_s = \begin{pmatrix} \bar{I}_o \\ \bar{I}_d \\ \bar{I}_i \end{pmatrix} = \frac{1}{3}\begin{pmatrix} 1 & 1 & 1 \\ 1 & \alpha & \alpha^2 \\ 1 & \alpha^2 & \alpha \end{pmatrix}\begin{pmatrix} \bar{I}_a \\ \bar{I}_b \\ \bar{I}_c \end{pmatrix}. \tag{3}$$

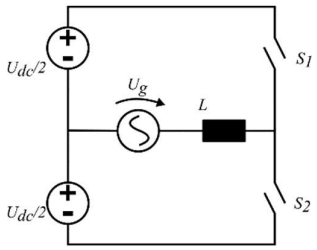

Fig. 7 Converter leg modulation. In a four-wire system the legs are independently controlled, therefore only one leg is shown.

The low frequency ripple on the dc capacitors due to grid imbalance has already been derived for the conventional non-isolated inverter in [9], and is the same for both power conversion directions, and reactive power. By including the turns ratio and neglecting the duty cycle loss during leg commutations, the same equation can be applied to the isolated HFLC. The peak to peak voltage ripple over a quarter of a grid period can be calculated as

$$\Delta V_{Cpp} = \frac{3M\left|\bar{I}_i\right|2n}{8\pi \cdot C_{dc}}, \tag{4}$$

where ΔV_{Cpp} is the peak to peak value of the low frequency ripple, M is the modulation index $|\bar{I}_i|$ is magnitude of the inverse component of the current, n is the turns ratio the transformer, f is the grid frequency and C_{dc} is the dc side capacitance.

The limit of the negative sequence current is determined by the permissible ripple on the dc side and the capacitance of the dc bus. To allow for greater unbalanced operation, the dc bus capacitance needs to be grossly oversized with respect to the balanced condition, and this would likely mean moving from film capacitors for switching ripple to electrolytic capacitors for unbalance ripple. In the extreme case, where only one phase operates at its nominal power, it is essentially a single phase inverter and must have a commensurately sized dc capacitance.

A contour plot that gives the voltage ripple percentage for different values of dc capacitance and inverse sequence current is shown in Fig. 8.

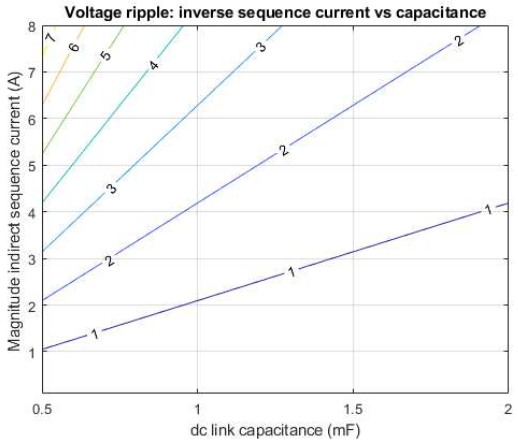

Fig 8. Contour plot of indirect sequence current and dc link capacitance giving the resulting voltage ripple percentage of the dc link, with modulation index M equal to 0.82.

TABLE I
HFLC SIMULATION PARAMETERS

Line to neutral voltage	230V RMS
dc side voltage	400V
Converter Power	3 2 kW
Grid inductance	1.3 mH
dc capacitance (balanced)	5 µF
dc capacitance (unbalanced)	1.3 mF
Turns ratio	1:1:1
Switching Frequency	50 kHz

IV. SIMULATION STUDY

The converter and its modulation were verified by a simulation model in PSIM. The simulation parameters are shown in Table I. Both operation under balanced and unbalanced currents was simulated, to show the effect of unbalanced currents on the ripple seen by the dc link.

In balanced operating conditions, where each phase has the same reference current, the average power across switching periods is constant, and the capacitor only need to filter the switching ripple. In fact, due to the practical interleaving effect described earlier, the filters actually operate with a frequency twice that of the switching. The balanced condition operation is shown in Fig. 9 (a) shows the balanced grid currents. There is some distortion in the current near the zero crossing due to the bidirectional switches, which block current in one direction and with the described modulation cannot effectively follow the current reference once it is below the average ripple current. Fig. 9 (b) instead shows the ripple on the passive components. T_1 and T_2 refer to the dc side full bridge, where during T_1 the dc side full bridge applies positive voltage, and negative voltage is applied during T_2. As previously shown, the ripple on the

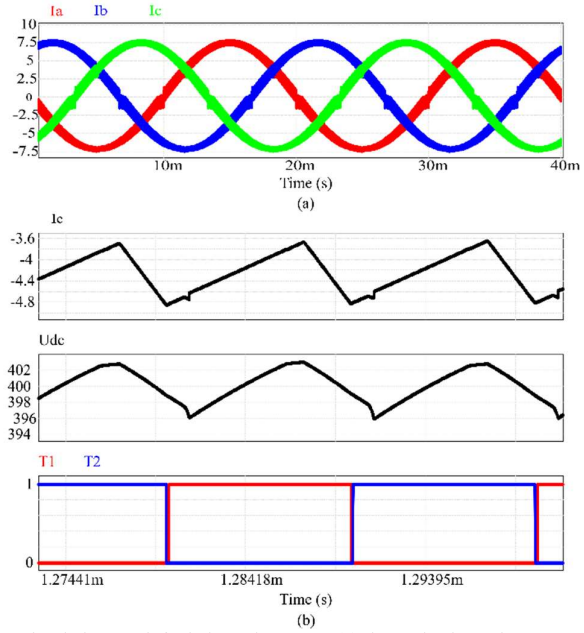

Fig. 9 Simulation result for balanced currents. (a) shows the three phase currents for two grid periods, (b) shows the switching characteristics of the capacitor voltage and grid inductor current for three switching periods. Ic is the current in phase c, Udc is the dc side capacitor voltage, and T1 T2 are the control signals for the full bridge on the dc side.

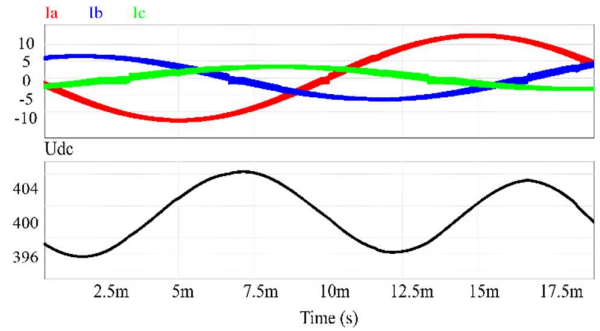

Fig. 10 Simulation result for unbalanced currents. The switching ripple is negligible in comparison to the 100 Hz ripple.

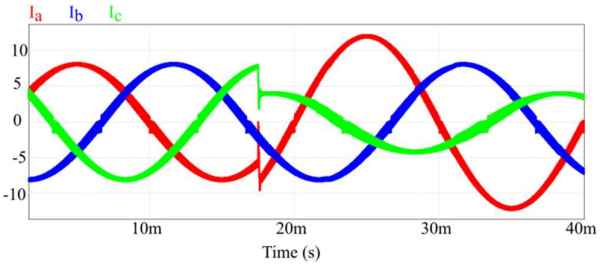

Fig. 11 Simulation of step response, from balanced to unbalanced operating condition.

passive components happens for every half-wave of the dc side voltage, meaning it is at double the switching frequency.

In order to be able to provide active phase balancing the converter must be able to operate with different current references. In the case of the center tapped transformer HFLC this is easily possible as the converter legs can be controlled as three independently controlled half-bridges. However, the previously described 100 Hz ripple will be present. The converter is simulated with reference current amplitudes $I_a = 12$ A, $I_b = 6$ A, and $I_c = 3$A. This gives an inverse sequence component with modulus of 2.65.

The imposed modulation index is 0.82. To filter the 100 Hz ripple the dc side capacitance is 1.3 mF. According to (4) this will give a peak to peak ripple of 8V, or 1% for 400 V. The converter operates as a rectifier to a 3.2 kW load. The simulation result is shown in Fig. 10, and is coherent with the calculated value.

The step response from balanced to unbalanced operation is shown in Fig. 11. The inherent strong dynamic performance of predictive digital controllers allows for very good step response to a change in the current references.

V. Conclusion

In this paper, the isolated high frequency converter is evaluated as the dc grid-forming converter in residential applications. The advantages and capabilities made possible by introducing a neutral wire connection are evaluated. The center-tapped three-phase high-frequency link converter is capable of unbalanced grid current operation, without increasing the number of semiconductor devices. However, the voltage stress on the ac-side devices is increased, while the operation under unbalanced conditions introduces a 100 Hz ripple on the dc voltage. The modulation method effectively doubles the switching frequency seen by the passive components, reducing the filtering effort. The converter is capable of providing grid balancing services, as the introduction of a center tap allows for full independent control of the currents.

Acknowledgment

This work was supported in part by the European Union's Horizon 2020 research and innovation programme under the Marie Sklodowska-Curie grant agreement no. 955614 and in part by the Estonian Research Council grant PRG1086.

References

[1] E. L. Carvalho, A. Blinov, A. Chub, P. Emiliani, G. de Carne, and D. Vinnikov, "Grid Integration of DC Buildings: Standards, Requirements and Power Converter Topologies," *IEEE Open J. Power Electron*., vol. 3, pp. 798–823, 2022, doi: 10.1109/OJPEL.2022.3217741.

[2] G. Makarabbi, V. Gavade, R. Panguloori, and P. Mishra, "Compatibility and performance study of home appliances in a DC home distribution system," in 2014 IEEE International Conference on Power Electronics, Drives and Energy Systems (PEDES), Mumbai, India: IEEE, Dec. 2014, pp. 1–6. doi: 10 1109/PEDES 2014.7042151.

[3] D. Kumar, F. Zare, and A. Ghosh, "DC Microgrid Technology: System Architectures, AC Grid Interfaces, Grounding Schemes, Power Quality, Communication Networks, Applications, and Standardizations Aspects," *IEEE Access*, vol. 5, pp. 12230–12256, 2017, doi: 10.1109/ACCESS.2017.2705914.

[4] J. Gallardo-Lozano, E. Romero-Cadaval, V. Miñambres-Marcos, D. Vinnikov, T. Jalakas and H. Hõimoja, "Grid reactive power compensation by using electric vehicles," 2014 Electric Power Quality and Supply Reliability Conference (PQ), Rakvere, Estonia, 2014, pp. 19-24, doi: 10.1109/PQ.2014.6866776.

[5] F. Flores-Bahamonde, H. Renaudineau, A. M. Llor, A. Chub and S. Kouro, "The DC Transformer Power Electronic Building Block: Powering Next-Generation Converter Design," in *IEEE Ind. Electron. Mag*., vol. 17, no. 1, pp. 21-35, March 2023, doi: 10.1109/MIE.2022.3147168.

[6] O. Korkh, A. Blinov, D. Vinnikov, and A. Chub, "Review of Isolated Matrix Inverters: Topologies, Modulation Methods and Applications," *Energies*, vol. 13, no. 9, p. 2394, May 2020, doi: 10.3390/en13092394.

[7] S. Norrga, S. Meier, and S. Ostlund, "A Three-Phase Soft-Switched Isolated AC/DC Converter Without Auxiliary Circuit," IEEE Trans. Ind. Appl., vol. 44, no. 3, pp. 836–844, 2008, doi: 10 1109/TIA.2008.921430.

[8] L. Schrittwieser, M. Leibl, and J. W. Kolar, "99% Efficient Isolated Three-Phase Matrix-Type DAB Buck–Boost PFC Rectifier," I*EEE Trans. Power Electron.*, vol. 35, no. 1, pp. 138–157, Jan. 2020, doi: 10.1109/TPEL 2019.2914488.

[9] P. Emiliani, A. Blinov, A. Chub, G. De Carne, and D. Vinnikov, "DC Grid Interface Converter based on Three-Phase Isolated Matrix Topology with Phase-Shift Modulation," in 2022 IEEE 13th International Symposium on Power Electronics for Distributed Generation Systems (PEDG), Kiel, Germany: IEEE, Jun. 2022, pp. 1–6. doi: 10.1109/PEDG54999.2022.9923256.

[10] M. Ucar, E. Ozdemir, and M. Kale, "An analysis of three-phase four-wire active power filter for harmonic elimination reactive power compensation and load balancing under nonideal mains voltage," in 2004 IEEE 35th Annual Power Electronics Specialists Conference (IEEE Cat. No.04CH37551), Aachen, Germany: IEEE, 2004, pp. 3089–3094. doi: 10.1109/PESC.2004 1355329.

[11] X. Pei, W. Zhou, and Y. Kang, "Analysis and Calculation of DC-Link Current and Voltage Ripples for Three-Phase Inverter With Unbalanced Load," *IEEE Trans. Power Electron*., vol. 30, no. 10, pp. 5401–5412, Oct. 2015, doi: 10.1109/TPEL.2014.2375353.

[12] A. Blinov, I. Verbytskyi, D. Peftitsis and D. Vinnikov, "Regenerative Passive Snubber Circuit for High-Frequency Link Converters," in *IEEE IEEE J. Emerg. Sel. Top. Power Electron.*, vol. 3, no. 2, pp. 252-257, April 2022, doi: 10.1109/JESTIE.2021.3066897.